

ULTRASTRUCTURAL ANALYSIS OF THE INTERACTION BETWEEN *Puccinia striiformis* f.sp. *tritici* AND WHEAT AFTER THERMAL INDUCTION OF RESISTANCE

Q. Ma and H.S. Shang

College of Plant Protection, Northwest Sci-Tech University of Agriculture and Forestry, Yangling, Shaanxi 712100, China

SUMMARY

Wheat cultivars with high-temperature resistance shortly exposed to 21°C expressed resistance to stripe rust, *Puccinia striiformis* f.sp. *tritici*, after being inoculated with the virulent strain CY29. Observations on the ultrastructural interactions between wheat and the rust fungus demonstrated that marked changes took place in both the fungus and the host mesophyll cells in resistance expression. Hyphae of the fungus were inhibited, and organelles developed vacuoles and disintegrated or collapsed. Development of haustorial mother cells and haustoria was retarded, and these were malformed and necrotized. The extrahaustorial membrane was stained more deeply, wrinkled, and perforated. The extrahaustorial matrix was widened and was coated with large amounts of electron-dense material. Host cells produced defense structures and material related to infection as well as hypersensitive responses. Formation of cell wall appositions, collars or papillae, and encasements of haustoria were essentially observed. In the interaction of the same wheat cultivars with the stripe rust avirulent strain (CY29-mut3) at normal temperature (16°C), the intracellular symptoms of incompatibility were similar to those of thermal induction. In the compatible interaction at 16°C, the pathogen was normal and there were no signs of disorganization or necrosis of infected host cells.

Key words: *Triticum aestivum*, *Puccinia striiformis* f.sp. *tritici*, interaction, resistance, cytology.

INTRODUCTION

Wheat stripe rust, caused by *Puccinia striiformis* West. f.sp. *tritici*, is one of the most destructive diseases of wheat, *Triticum aestivum* L., worldwide. It is generally accepted that growing resistant cultivars is the most effective and essential method to control the disease. As

the loss of resistance in race-specific wheat cultivars becomes more and more serious, however, cultivars with high-temperature durable resistance have received increasing attention (Line, 1983).

The concept of high-temperature, adult-plant resistance (HTAR) of wheat to stripe rust was first put forward by Qayoum and Line (1985). It is known that expression of the resistance gene *Sr6* is temperature dependent in wheat resistant to *Puccinia graminis* Pers. f.sp. *tritici* Eriks. et Henn. Stem rust resistant plants carrying the *Sr6* gene display an incompatible reaction at 19°C, but develop susceptible-type reactions at about 26°C (Harder *et al.*, 1979). HTAR is the opposite, the expression of the resistance being at temperature higher than that optimal for the disease (16°C). HTAR is an induced low-infection type resistance according to Stakman *et al.* (1962). Our previous studies on HTAR of wheat to stripe rust revealed that: i) the minimum temperature inducing the resistance varied from 18 to 21°C among different wheat cultivars; ii) the minimum lengths of thermal treatment varied from 8 to 12 h; iii) the optimal time for thermal treatment was before the symptoms appeared; iv) only post-inoculation thermal induction was effective, while pre-inoculation treatment was of no effect (Shang *et al.*, 1997; Wang *et al.*, 1996).

Our preliminary histopathological studies with fluorescence light microscopy showed that HTAR has the characteristics of the hypersensitive response (Shang, 1998), but fungal development and host responses at cytological level were not clear in HTAR expression. Therefore, to reveal the mechanisms of HTAR, the ultrastructural characters of host-pathogen interaction in the expression of the resistance were examined by transmission electron microscopy in high-temperature resistant wheat cultivars, inoculated with *P. striiformis*, and submitted to thermal induction.

MATERIALS AND METHODS

Pathogen and host. A Chinese strain (CY29) and its UV-induced avirulent mutant (CY29-mut3) of *P. striiformis* were used in this study. Uredospores were produced on a susceptible wheat cultivar Mingxian 169

with no resistant genes. CY29-mut3, used as incompatible control, had the same genetic background with CY29, differing only in lack of virulence.

Wheat (*T. aestivum*) cvs. Xiaoyan 6 and Lantian 1, with typical HTAR to stripe rust, were used. Wheat seeds were sown in organic soil in 10 cm pots in a growth chamber at 16°C and with a 16 h photoperiod. Eight-day-old seedlings were used for inoculation when the primary leaves were fully expanded.

Inoculation and thermal induction. Freshly collected uredioconidia were applied with a fine paintbrush to the adaxial surface of the first leaf of wheat seedlings. Inoculated seedlings were kept in a humid chamber for 24 h at 16°C in the dark, and were then moved back to the growth chamber. For thermal induction, some of the plants inoculated with CY29 were kept at 21°C for 24 h in standard long day conditions until symptom appearance, and then returned to the growth chamber at 16°C. The other plants inoculated with CY29 or CY29-mut3, as compatible and incompatible controls, were always kept at the control temperature (16°C).

Transmission electron microscopy. In both thermal-induced and control plants, inoculated leaves were sampled 12, 24, and 48 h after lesions appeared. Samples were cut into small pieces and fixed with 3% (v/v) glutaraldehyde in 50 mM phosphate buffer (pH 6.8) for 16 h at 4°C, rinsed thoroughly with the same buffer, and post-fixed with 1% (w/v) osmium tetroxide for 2 h at 4°C. The samples were, then, dehydrated in a graded acetone series, embedded in Epon-araldite and kept 1 day at 60°C for polymerisation. Ultra-thin sections of the samples were cut with a diamond knife and placed on 200-mesh copper grids. After contrasting with uranyl acetate and lead citrate, the grids were examined with JEM-200EX electron microscope at 80 KV.

RESULTS

The infection process of *P. striiformis* in wheat is similar to that of other cereal rusts, including the formation of substomatal vesicles, intercellular hyphae, haustorial mother cells, and haustoria. The high-temperature resistant cultivars Xiaoyan 6 and Lantian 1 inoculated with CY29 expressed compatible reactions to the fungus at 16°C. The thermal induction at 21°C when the leaves started to show lesions, however, transformed the reaction from compatibility to incompatibility, resulting in HTAR expression. At the control temperature (16°C), the leaves of cvs. Xiaoyan 6 and Lantian 1 were extensively colonized when lesions appeared. Fungal hyphae, developed in the intercellular spaces between mesophyll cells, contained numerous ribosomes, mitochondria, endoplasmic reticulum and nuclei (Fig. 1A). The haustori-

um consisted typically of a neck and a body. Generally, no obvious adverse effects were detected in the host cells after haustorium formation, although the host cell nucleus and other organelles were often associated with the haustorial body (Fig. 1B). The extrahaustorial matrix was narrow, with none or just a little material deposited (Fig. 1C). An electron-opaque neckband was observed along the haustorial neck (Fig. 1D). One of the common host responses observed was the deposition of electron-dense material, namely collar around the haustorial neck in some of the infected host cells (Fig. 1D).

After thermal induction at 21°C for 12 h, both the pathogen and the host cells displayed notable changes at the ultrastructural level, and the host formed resistance-related structures and materials. A few hyphal cells showed abnormalities in the infected leaves of both cvs. Xiaoyan 6 and Lantian 1. Many small vacuoles appeared in the cytoplasm; organelles, such as mitochondria, became vacuolated, and many electron-dense granular deposits were present (Fig. 2A). Unique dark materials appeared between the host cells and the hyphae on a few occasions (Fig. 2B), but it was not clear whether such materials were from the pathogen or the host cells. The haustorial mother cell walls became thickened, and electron-dense, dark lipid-like materials often appeared around the large vacuoles, and lost their ability to produce penetration structures (Fig. 2C). Some haustorial bodies were unable to expand normally and were malformed with angular outlines, electron-dense protoplasm and organelles became disorganized, dark lipid-like materials often appeared around the large vacuoles (Fig. 2D). Another marked change in haustoria in thermal-induced infected leaves was a widening of the extrahaustorial matrix with electron-dense fibrillar and granular materials. The extrahaustorial membrane became wrinkled and perforated (Fig. 2E). The thickness of the haustorial walls was markedly thickened, 2 to 3 times thicker than that of the haustorium at control temperature. In Lantian 1 the inhibition was more serious, the thickness of haustorium walls being 4-5 times thicker and more densely stained than that at control temperature (Fig. 2F).

One of the early host responses observed after thermal induction was the apposition of electron-dense materials on the inner surface of host cell walls, directly in contact with intercellular hyphae or haustorial mother cells. These appositions were electron-opaque, quite variable in size, and often had a layered appearance, leading to invagination of the plasmalemma (Fig. 3A). Fungal attempts to penetrate host cells were apparently retarded and accompanied by formation of a papilla-like material that was formed opposite the thickened area of the haustorial mother cells from which the penetration peg would normally have arisen (Fig. 3B). The host cell wall was penetrated, but further development of the haustorium was stopped by the papilla. Callose

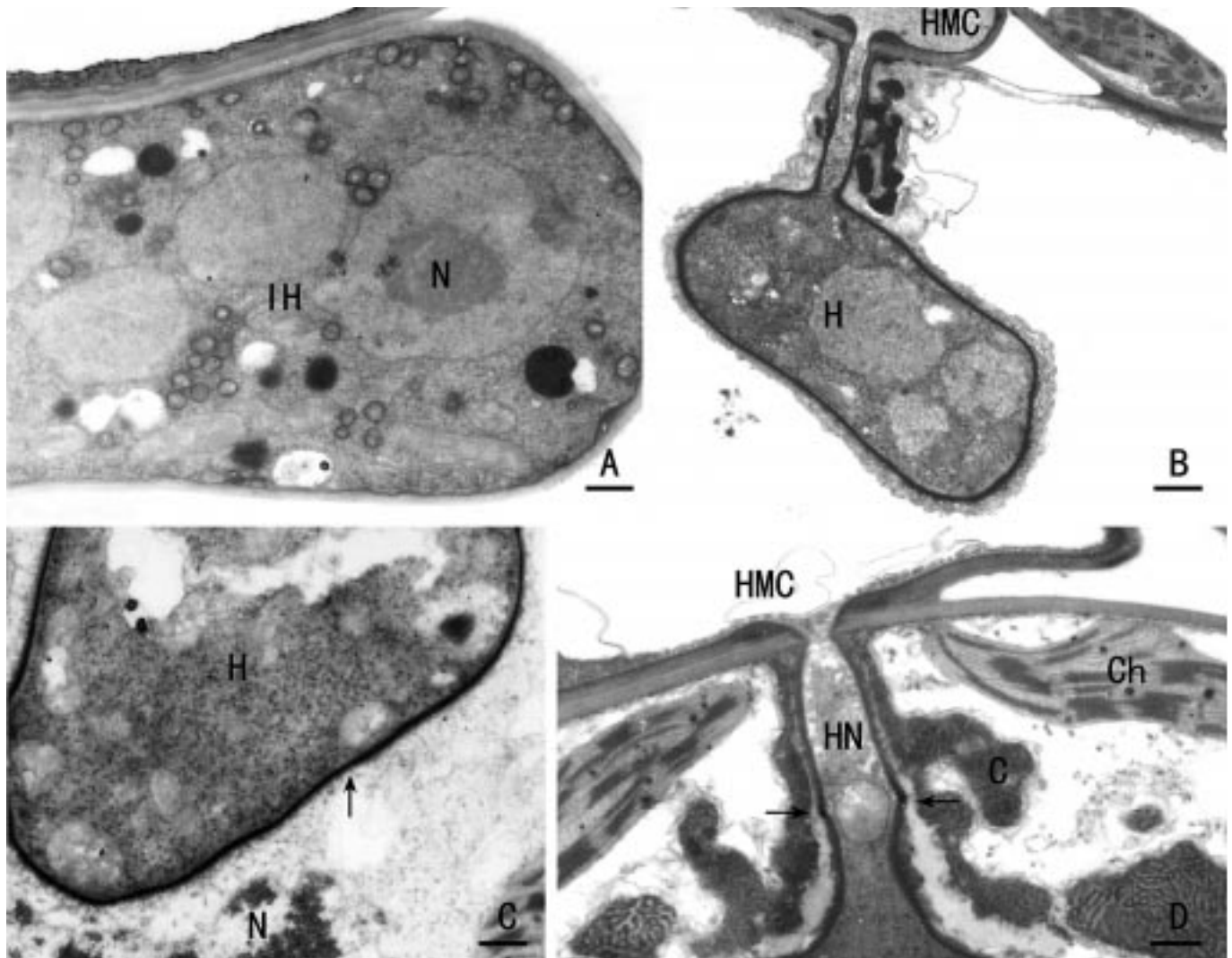


Fig. 1. Transmission electron micrographs of fungal development and host cell responses in infected wheat leaves in compatible combination at control temperature (16°C). **A)** Intercellular hypha with nuclei. Bar=1 µm. **B)** A mature haustorium in the host cell consisting of haustorial neck and haustorial body. Bar=1 µm. **C)** Extra-haustorial matrix (arrowhead) with no or just a little material deposited. Bar=0.5 µm. **D)** A penetration site and haustorial neck: an electron-dense ring surrounds the neck (arrowheads) and a collar formed around the haustorial neck. Bar=0.5 µm. IH: intercellular hypha; N: nucleus; H: haustorium; HN: haustorial neck; HMC: haustorial mother cell; Ch: chloroplast; C: collar.

also formed opposite the fungal penetration (Fig. 3C).

After 12 h at 21°C, the host plasmalemma was densely stained and the cytoplasm became vesiculated in a few invaded mesophyll cells. There were accumulations of electron-dense material along the membranes of the vacuoles, but not the haustorium; at this time, the host cells necrotized completely, as shown in Fig. 3D. After 24 h at 21°C, the number of such cells increased, but the organelles were still observable at various disintegrated stages. Vacuolar membranes crinkled and were disintegrated. The mitochondria were rounded, and had disorganized cristae, and their double membrane was disrupted and became vesiculated. Chloroplasts were swollen, deformed, and electron-dense with indistinct lamellae (Fig. 3E). Some of the thylakoid stacks ap-

peared to have coalesced, with their membranes ruptured, and lamellae dispersed in the cytoplasm (Fig. 3F). Endoplasmic reticulum within host cells was irregular in shape, and gradually vesiculated. The nuclei no longer showed the uniform and relaxed structure, which indicates an active metabolic state, the nuclear matter becoming irregular and coagulated. The rest of the cytoplasm was highly vesiculated. Changes in the host protoplasm were accompanied by invagination, folding and disruption of the cytoplasm. The haustoria in these host cells were also disintegrated and necrotic. There were a number of vacuoles of various sizes in the cytoplasm, and only some of the thylakoid stacks of the chloroplasts and necrotized haustoria were recognizable (Fig. 3F). The cell walls became loosened in structure, and cavities

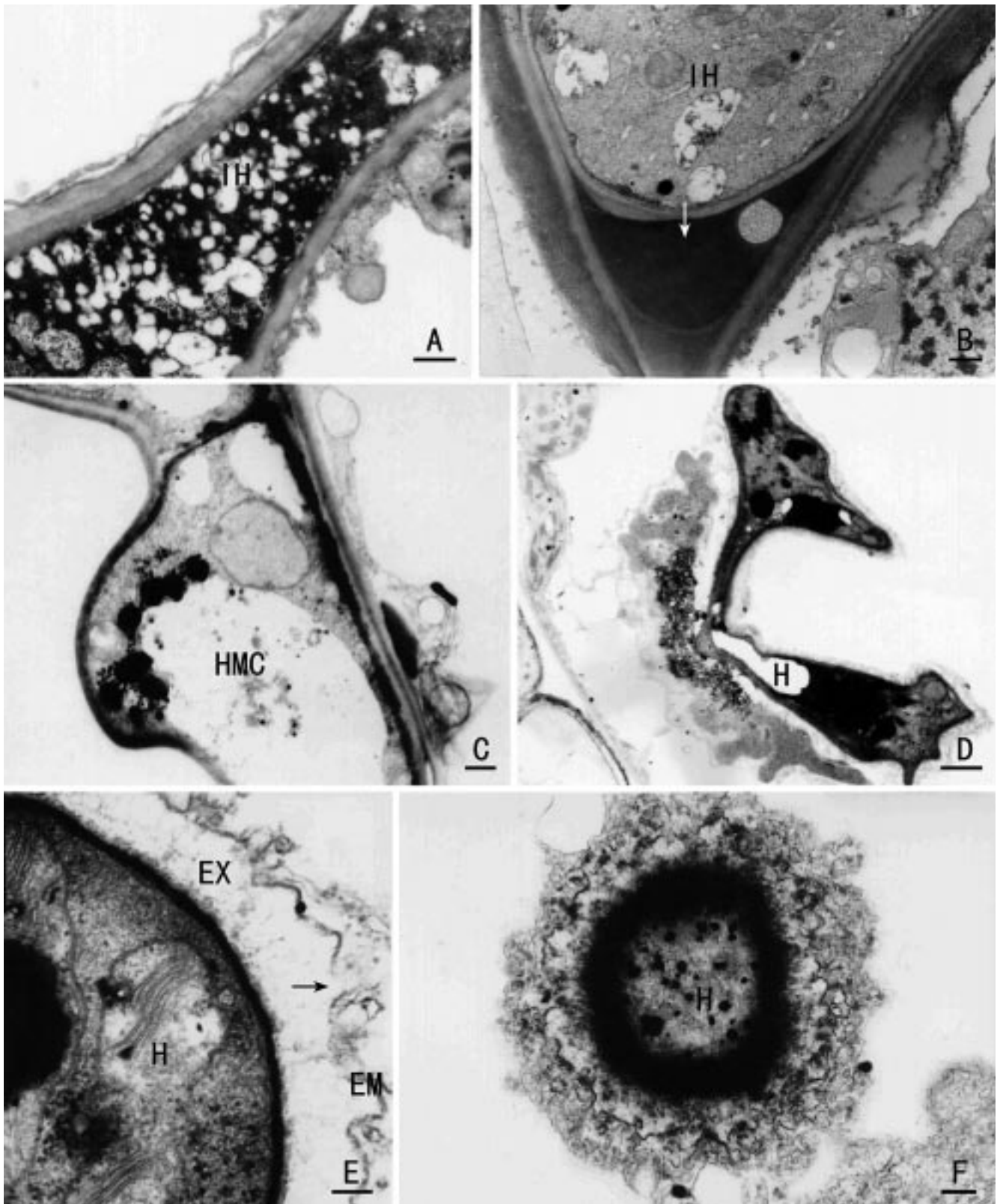


Fig. 2. Transmission electron micrographs of fungal development and host cell responses in infected wheat leaves in incompatible combination induced by high-temperature treatment. **A)** Intercellular hypha vesicularized, disintegrated, and necrotized. Bar=0.5 μm . **B)** Dark materials appeared between host cells and hyphae (arrowhead). Bar=0.4 μm . **C)** Haustorial mother cell vacuolated with deeply stained lipid material. Bar=0.5 μm . **D)** Malformed, vacuolated haustorium with lipid-like material. Bar=1 μm . **E)** Extrahaustorial membrane wrinkled and perforated (arrowhead), extrahaustorial matrix thickened with electron-dense material deposited. Bar=0.1 μm . **F)** Haustorial wall thickened greatly. Bar=0.25 μm . IH: intercellular hypha; H: haustorium; HMC: haustorial mother cell; EM: extrahaustorial membrane; EX: extrahaustorial matrix.

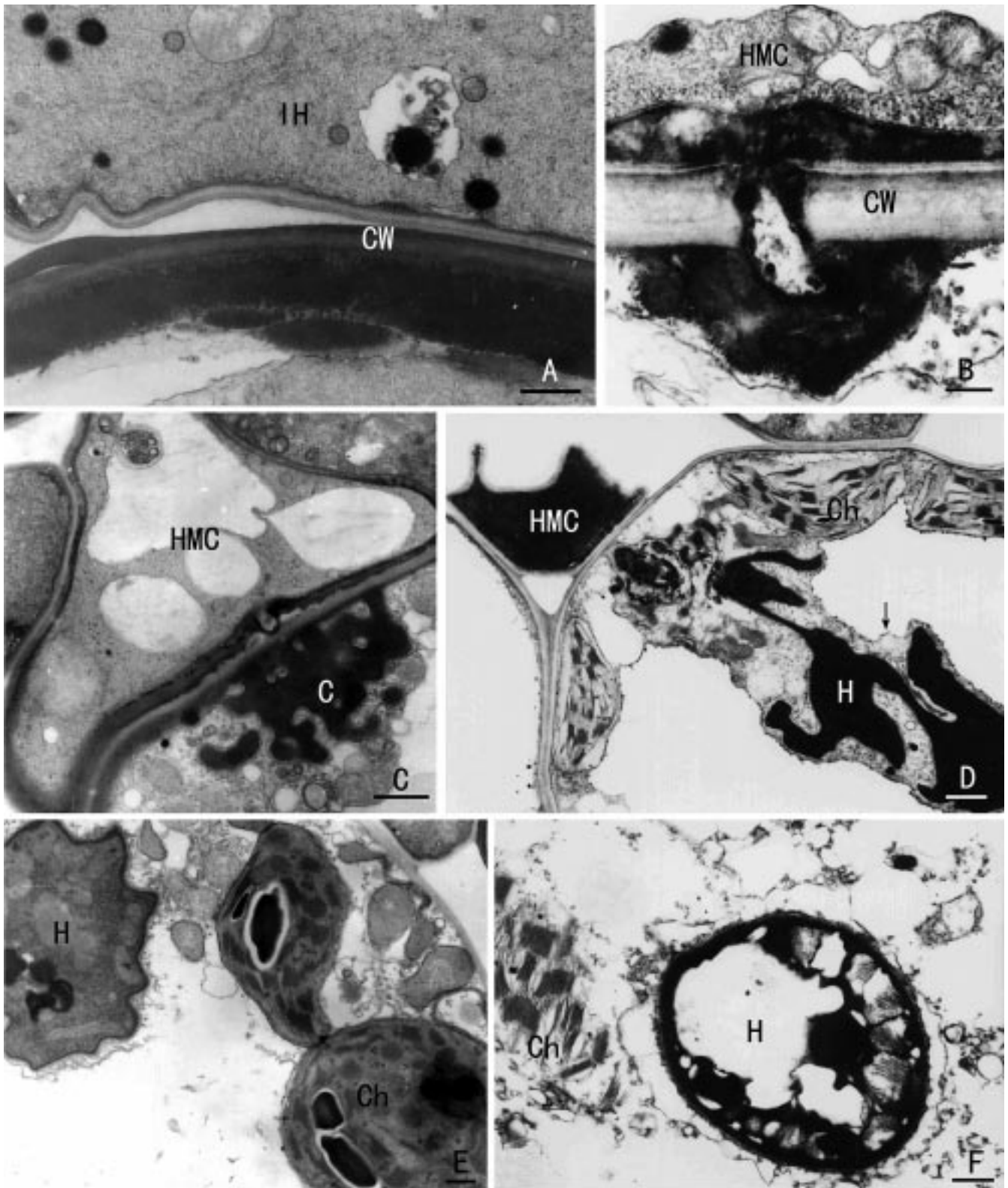


Fig. 3. Transmission electron micrographs of fungal development and host cell responses in infected wheat leaves in incompatible combination under high-temperature treatment. **A)** Deposition of electron-dense materials on the inner surface of the host cell wall in contact with intercellular hyphae. Bar=0.5 μ m. **B)** Papilla-like apposition between host cell wall and plasmalemma at penetration site. Bar=0.2 μ m. **C)** Callose formed opposite the fungal penetration peg. Bar=1 μ m. **D)** Electron-dense material along the membranes of vacuoles, the haustorium is necrotized while the host cell still appears living (arrowhead). Bar=1 μ m. **E)** Swollen, deformed, and electron-dense chloroplasts. Bar=0.5 μ m. **F)** Host organelles disintegrated, only some of the thylakoid stacks were recognizable in chloroplasts, the haustorium also disintegrated and necrotic. Bar=0.5 μ m. CW: host cell wall; IH: intercellular hypha; HMC: haustorial mother cell; C: callose; H: haustorium; Ch: chloroplast.

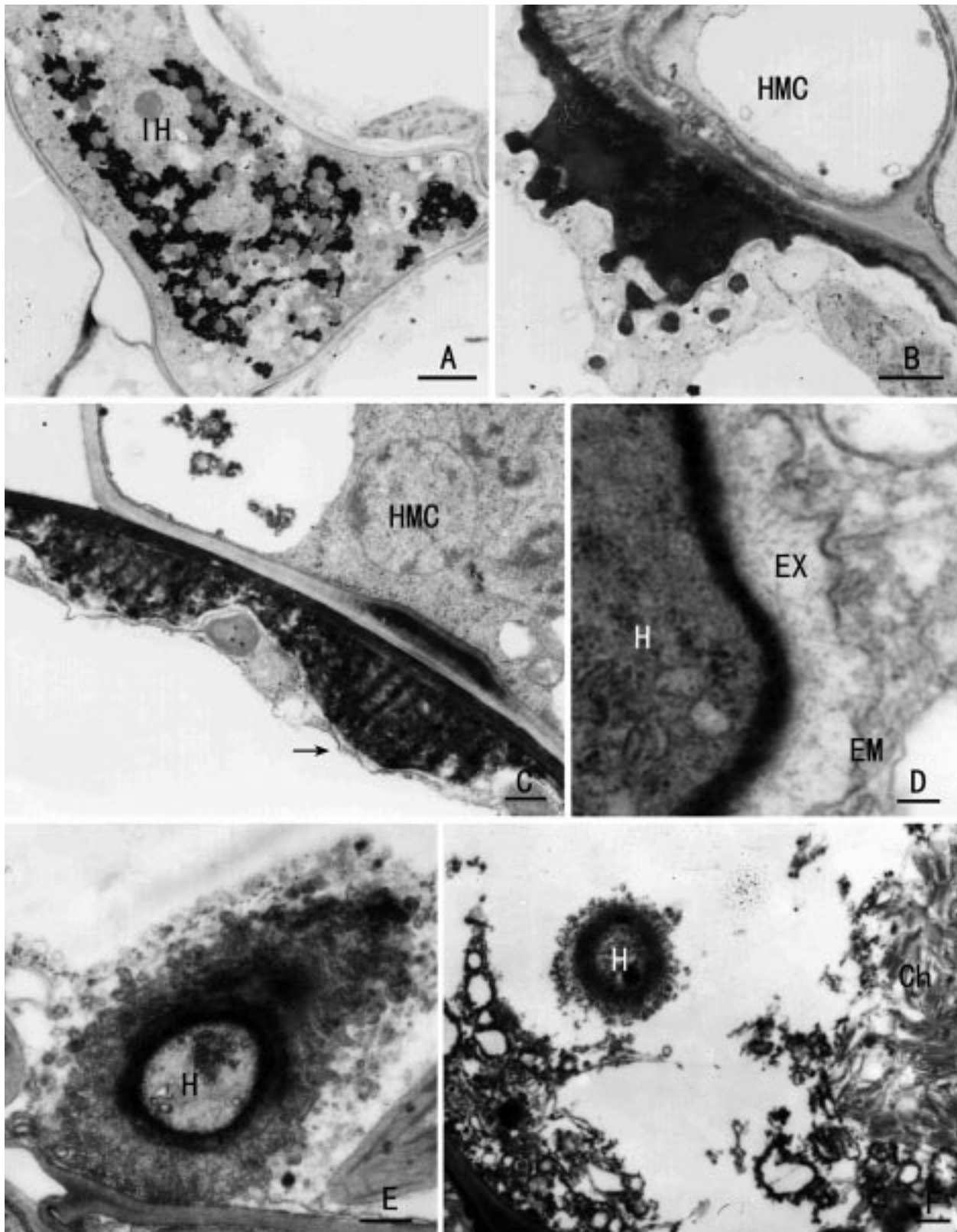


Fig. 4. Transmission electron micrographs of fungal development and host cell responses in infected wheat leaves in incompatible combination at control temperature treatment. **A)** Intercellular hypha disorganized and containing electron-dense granular materials. Bar=2 μ m. **B)** Papilla-like apposition between host cell wall and plasmalemma at penetration site. Bar=1 μ m. **C)** Deposition of electron-dense materials on the inner surface of the host cell wall in contact with haustorial mother cell (arrowhead). Bar=0.5 μ m. **D)** Extrahaustorial matrix thickened with electron-dense material deposited. Bar=0.2 μ m. **E)** Haustorium encased by electron-dense material. Bar=0.5 μ m. **F)** Host cell necrotic, and the haustorium also. Bar=0.5 μ m. IH: intercellular hypha; H: haustorium; EX: extrahaustorial matrix; EM: extrahaustorial membrane; CW: host cell wall; HMC: haustorial mother cell.

appeared. Eventually, the host wall disintegrated. The neighbouring uninfected cells contacting with necrotic host cell were also affected. The plasmolysis occurred gradually in the neighbouring cells, and their cell wall became electron-dense, and dark material appeared between the host wall and plasmalemma. Gradually, the cytoplasm became vesiculated and necrotic. In an advanced stage of thermal induction, more necrotic host cells were detected in infected leaves and the intercellular hyphae were necrotic or collapsed, indicating that fungal development had ceased.

In incompatible interactions between cvs. Xiaoyan 6 and Lantian 1 and the hypovirulent mutant CY29-mut3 at control temperature (16°C), the fungal development was markedly restricted in infected leaves. The inhibition of the intercellular hyphae, haustorial mother cells, and haustoria were like those observed in thermal-induced leaves inoculated with the virulent strain CY29. Intercellular hyphae were vesiculated and disorganized with electron-dense granular materials (Fig. 4A). Sometimes, a papilla-like material was formed in the infected host cell at the penetration site in response to the penetration peg of the haustorial mother cells (Fig. 4B). Electron-dense material was deposited on the inner surface of host cell walls directly in contact with intercellular hyphae or haustorial mother cells (Fig. 4C). The widening of the extrahaustorial matrix with electron-dense fibrillar and granular materials were also visible (Fig. 4D). Sometimes, the haustorium was encased by electron-dense material (Fig. 4E), and the haustorial body collapsed and became necrotic while the host cell was unaffected. In addition, necrosis of host cells was observed in all infection sites. The death of host cells in which haustoria had been produced was accompanied by necrosis of the haustoria (Fig. 4F). Later, the neighbouring uninfected host cells also became necrotic, and the fungal development was arrested.

DISCUSSION

Our studies demonstrate that fungal development and host responses in HTAR expression is similar to that of the typical incompatible interaction of wheat with stripe rust. The fungal development in wheat leaves was markedly restricted and structural defense reactions and hypersensitive responses of the host occurred. Structural defense reactions, such as formation of cell wall apposition, collar or papilla, and haustorium encasement were more markedly produced in the infected leaves of thermally induced plants than in the compatible combination. At the penetration sites, the papilla-like apposition under the host cell wall might resist the invasion of the rust fungus; this in a way is similar to that of the incompatible combination of wheat with *P. striiformis*. Jacobs (1989) reported that aborted

infection structures in *P. recondita*-infected leaves of partially resistant wheat cultivars were associated with abundant cell wall appositions, suggesting that the formation of cell wall appositions was one of the resistance mechanisms for partial resistance of wheat to leaf rust. In incompatible combinations, β -1,3-glucanase activity within host wall and wall deposits is higher than that in the compatible interaction (Hu, 1998). In the present study, the cell wall appositions in infected leaves were rarely detected in the compatible combination, although collars were formed in some infected host cells during haustorium formation. In contrast, in HTAR and incompatible combination, very thick layers of cell wall appositions were often detected in host cells in contact with haustorial mother cells and intercellular hyphae. The formation of cell wall appositions constitutes an additional physical barrier, contributing to host wall strength and restriction of the pathogen's colonization.

The necrotic response of the host cells, often occurring during haustoria formation, is a common phenomenon in HTAR and incompatible combinations, but does not occur in heat-treated and non-inoculated resistant or susceptible plants. In HTAR, some of the haustorium-bearing host cells remained alive in infected host tissues although the haustoria were necrotic in these host cells, as has been found in other rusts-cereal incompatible combinations (Skipp *et al.*, 1974; Prusky *et al.*, 1980). This indicates that death of the haustorium of *P. striiformis* being not always the consequence of host cell necrosis (Wang, 1996; Ma and Shang, 2002).

The structure of the extrahaustorial membrane also showed marked changes in the course of HTAR expression, the main characters of which included the membrane becoming electron-denser, wrinkled and perforated. In a similar way, the extrahaustorial matrix was thickened and infiltrated with electron-dense fibrillar material. All these changes might play roles in the exchanges of material between the host and the rust fungus.

Prior to peg penetration into a host cell, the host showed the same defense reaction characteristics as with the incompatible combination before and after haustorium formation. The events determining HTAR must precede the occurrence of the defense reaction, and should occur during the recognition process. Biochemical studies reveal that at the early stages of HTAR expression, activity of key enzymes for the synthesis of lignin increase markedly, lignin accumulates rapidly, and pathogenesis-related proteins of various molecular weights accumulate (Wang *et al.*, 1996; Shang, 1998). These changes correspond to the characters observed in the present studies, and could provide an important approach for clarifying the mechanisms of HTAR in wheat. The interactions between *Puccinia striiformis* f.sp. *tritici* and wheat, in earlier phases of infection after thermal induction, and molecular mechanisms involved remain to be investigated in the future.

REFERENCES

- Harder D.E., Rohringer R., Samborski D.J., Rimmer S.R., Kim W.K., Chong J., 1979. Electron microscopy of susceptible and resistant near-isogenic (*sr6/Sr6*) lines of wheat infected by *Puccinia graminis tritici*. II. Expression of incompatibility in mesophyll and epidermal cells and the effect of temperature on host-parasite interactions in these cells. *Canadian Journal of Botany* **57**: 2617-2625.
- Hu G.G., Rijkenberg F.H.J., 1998. Subcellular localization of β -1,3-glucanase in *Puccinia recondita* f.sp. *tritici*-infected wheat leaves. *Planta* **204**: 324-334.
- Hu G.G., Rijkenberg F.H.J., 1998. Ultrastructural studies of the intercellular hypha and haustorium of *Puccinia recondita* f.sp. *tritici*. *Journal of Phytopathology* **146**: 39-50.
- Jacobs T., 1989. Haustorium formation and cell wall appositions in susceptible and partially resistant wheat and barley seedlings infected with wheat leaf rust. *Journal of Phytopathology* **127**: 250-261.
- Jacobs T., van Hee, Engels F.M., 1993. The ultrastructure of the interface between susceptible, partially resistant spring wheat genotypes and wheat leaf rust. *Mededelingen Faculteit Landbouwkundige Universiteit Gent* **58**: 1-10.
- Line R.F., Qayoum A., Milus G., 1983. Durable resistance to stripe rust of wheat. In: *Abstracts of papers 4th International Congress on Plant Pathology, Melbourne, Australia*, 204.
- Ma Q., Shang H.S., 2002. Ultrastructure of an incompatible interaction between wheat and *Puccinia striiformis*. *Acta Phytopathologica Sinica* **32**(4): 306-311.
- Qayoum A., Line R.F., 1985. High-temperature, adult-plant resistance to stripe rust of wheat. *Phytopathology* **75**: 1121-1125.
- Prusky D., Dinoor A., Jacoby B., 1980. The sequence of death of haustoria and host cells during the hypersensitive reaction of oat to crown rust. *Physiology and Plant Pathology* **17**: 33-40.
- Shang H.S., 1998. High-temperature resistance of wheat to stripe rust. *Scientia Agricultura Sinica* **3**(4): 46-50.
- Shang H.S., Wang L.G., Lu H.P., Jing J.X., 1997. Characteristics of expression of high-temperature resistance to stripe rust in wheat. *Acta Phytophylacica Sinica* **24**(2): 97-100.
- Skipp R.A., Samborski D.J., 1974. The effect of the *Sr6* gene for host resistance on histological events during the development of stem rust in near-isogenic wheat lines. *Canadian Journal of Botany* **52**: 1107-1111.
- Stakman E.C., Stewart D. M., Loeqering W.Q., 1962. Identification of physiologic races of *P. graminis tritici*. USDA Agricultural Research Service E617.
- Wang B.T, Shang H.S., 1996. The relation between the high-temperature resistance of wheat to stripe rust and lignin synthesis. *Acta Phytophylacica Sinica* **23**(3): 229-234.
- Wang Y., 1996. Histology and cytology of wheat resistance of low reaction type to stripe rust. MSc Thesis, Northwest Agricultural University, China.

Received 4 February 2003

Accepted 12 February 2004